Original Article

Acupuncture and Herbal Medicine

OPEN

Development and evaluation of *Panax notoginseng* saponins contained in an *in situ* pH-triggered gelling system for sustained ocular posterior segment drug delivery

Peng Lu[1,2,3], Renxing Wang[1,2], Yue Xing[1,2], Yanquan Gao[1,2], Qingqing Zhang[1,2], Bin Xing[1,2], Ying Zhang[1,2], Changxiang Yu[1,2], Xinfu Cai[4,5], Qiang Shang[4,5], Dereje Kebebe[6,*], Jiaxin Pi[1,2,*], Zhidong Liu[1,2,*]

Abstract

Objective: This study aimed to lay the foundation for the research on *Panax notoginseng* saponins (PNS) in pH-sensitive *in situ* gel and the development and improvement of related preparations.

Methods: We used Carbopol®940, a commonly used pH-sensitive polymer, and the thickener hydroxypropyl methylcellulose (HPMC E4M) as an ophthalmic gel matrix to prepare an ophthalmic *in situ* gel of PNS. In addition, formula optimization was performed by assessing gelling capability with the results of *in vitro* release studies. *In vitro* (corneal permeation, rheological, and stability) and *in vivo* (ocular irritation and preliminary pharmacokinetics in the vitreous) studies were also performed.

Results: The results demonstrated that the *in situ* gelling systems containing PNS showed a sustained release of the drug, making it an ideal ocular delivery system for improving posterior ocular bioavailability.

Conclusions: This study lays the foundation for the research of PNS contained in an *in situ* pH-triggered gel as well as the development and improvement of related preparations. It concurrently traditional Chinese medicine with a contemporary *in situ* gelling approach to provide new directions for the treatment of posterior ocular diseases such as diabetic retinopathy.

Keywords: Carbopol®940, Hydroxypropyl methylcellulose, *Panax notoginseng* saponins, pH-triggered gelling system, Sustained release drug delivery

1 Introduction

A great number of previous studies have investigated the potential of *Panax notoginseng* saponins (PNS) for the treatment of various diseases[1–5], including posterior ocular diseases such as diabetic retinopathy (DR)[2,6–8]. PNS, the major active component of the widely used traditional Chinese medicine (TCM) *P. notoginseng* (Burk.) F. H. Chen[9], includes different saponins, such as ginsenoside Rg_1, ginsenoside Rb_1 and notoginsenoside R_1[10–11]. Various PNS preparations, such as Xueshuantong capsules[7,12] and Xueshuantong injection[8,13–14], have been commercially available and widely applied in clinics. However, PNS has poor oral bioavailability due to poor stability under gastric conditions, low membrane permeability, and high molecular weight[15–16]. In addition, to maintain the therapeutic efficacy, a long-term frequent intravenous administration is required, leading to poor patient compliance owing to the inconvenience caused by the administration route. Moreover, drugs that are administered systemically in the ophthalmic system are also recalcitrant to enter the eye tissues[17–18]. Therefore, a need remains to find a new alternative non-injection route of drug delivery system (such as ophthalmic delivery system) for the treatment of ocular diseases with PNS, especially posterior ocular diseases such as DR[5–6].

The eye is a complex and unique part of human organs, divided into two segments: anterior and posterior segments[18]. Many conditions, notably DR affect the posterior segment[19–20]. One of the main difficulties in ocular drug delivery is to achieve and retain the optimal drug concentration in the desired site of action within the eye. A number of ophthalmic dosage forms (ointments, eye drops, gels, and ocular inserts) have been investigated to extend the ocular residence time of drugs after the topical application[21]. There is an increase in the corneal

Peng Lu, Renxing Wang, and Yue Xing contributed equally to this work.

[1] State Key Laboratory of Component-Based Chinese Medicine, Tianjin University of Traditional Chinese Medicine, Tianjin, China; [2] Engineering Research Center of Modern Chinese Medicine Discovery and Preparation Technique, Ministry of Education, Tianjin, China; [3] Department of pharmacy, Suzhou TCM Hospital Affiliated to Nanjing University of Chinese Medicine, Suzhou, China; [4] Sichuan Guangda Pharmaceutical Co. LTD, Pengzhou, China; [5] Sichuan Engineering Research Center of Antiviral Traditional Chinese Medicine Industrialization, Pengzhou, China; [6] School of Pharmacy, Institute of Health, Jimma University, Jimma, Ethiopia.

[*] Corresponding author. Dereje Kebebe, School of Pharmacy, Institute of Health, Jimma University, Ethiopia, E-mail: Dereje.keborg@gmail.com; Jiaxin Pi, State Key Laboratory of Component-Based Chinese Medicine, Tianjin University of Traditional Chinese Medicine, Tianjin 301617, China, E-mail: pijiaxin@tjutcm.edu.cn; Zhidong Liu, State Key Laboratory of Component-Based Chinese Medicine, Tianjin University of Traditional Chinese Medicine, Tianjin 301617, China, E-mail: liuzhidong@tjutcm.edu.cn.

Acupuncture and Herbal Medicine (2021) 1:2

Received 29 July 2021 / Accepted 24 November 2021

http://dx.doi.org/10.1097/HM9.0000000000000020

contact time with these formulations. However, because of blurred vision and poor patient compliance, the ointments and inserts have not yet been fully accepted[22]. It is recommended to deliver drugs to the posterior of the eye *via* intravitreal and periocular routes[21,23]. However, these routes also have some disadvantages. For example, frequent intravitreal injections may cause pain and affect patient compliance. Thus, although the periocular routes of drug administration are easy and convenient, static, and dynamic barriers pose a problem[23].

Over the past few decades, various delivery systems have been developed, such as those using chemical permeability enhancers[17], prodrugs[24], and stimuli-responsive *in situ* gels[25–26] to increase ocular residence time, drug penetration across the ocular barriers, and ophthalmic bioavailability. *In situ* gelling systems are one of the promising ways to improve the retention time of drugs on the ocular surface[25–29]. After the instillation of an aqueous solution containing stimuli-responsive polymers such as pH-sensitive polymers[27], thermosensitive polymers[25–26], and ion-sensitive polymers[28–29], a vicious and mucoadhesive gel is formed on the ocular surface[30]. The ocular retention time and bioavailability of ophthalmic drugs are improved when delivered *via* this gel.

In this study, we used Carbopol®940, a commonly used pH-sensitive polymer and thickener hydroxypropyl methylcellulose (HPMC E4M) as an ophthalmic gel matrix to prepare the ophthalmic gel for PNS delivery *in situ*. We then performed *in vitro* (corneal permeation, rheological, and stability) and *in vivo* (ocular irritation and preliminary pharmacokinetic in the vitreous) studies to investigate the drug delivery system.

2 Methods

2.1 Materials and animals

Ginsenoside Rg_1 (batch number: 110703-201832, purity 92.4%), ginsenoside Rb_1 (batch number: 110704-201824, purity 92.49%), and notoginsenoside R_1 (batch number: 110745-201820, purity 93.1%) were all provided from National Institutes for Food and Drug Control (Beijing, China). *P. notoginseng* saponin bulk drug (batch number: 021108) was purchased from Yunnan Yuxi Wanfang Natural Medicine Co. (Yunnan, China). HPMC E4M (batch number: PDR457286) was provided by Shanghai Kalekang Coating Technology Co. (Shanghai, China). Carbopol®940 was purchased from Lubrizol Specialty Chemicals (Shanghai) Co. (Shanghai, China). Sodium chloride, sodium bicarbonate, potassium chloride, and magnesium chloride of analytical grade were provided by Tianjin Chemical Reagent Wholesale Co. (Tianjin, China). Sodium hydroxide and hydrated calcium chloride (both of analytical grade) were purchased from Tianjin Jinke Fine Chemical Research Institute (Tianjin, China). Ethylenediaminetetraacetic acid disodium salt (EDTA-2Na) and oxidized glutathione (batch No: Q14J8J39858) were provided by Shanghai Yuanye Biotechnology Co. (Shanghai, China). Potassium dihydrogen phosphate and glucose were purchased from Tianjin Sailboat Chemical Reagent Technology Co. (Tianjin, China). Acetonitrile and methanol of HPLC grade were provided by Fisher Scientific Co. (Fairlawn, NJ, USA). Ultrapure water was obtained from a Milli-Q water purification system (Millipore, USA).

Twelve New Zealand white rabbits with half males and females, weighing 2–2.5 kg, were provided by The Chinese Academy of Medical Sciences of Radiation Research Institute (License: SCXK JIN 2010-0004, Tianjin, China). Before the experiment, animals were fasted for 12 h and were given free access to water.

2.2 Solubility, stability, and apparent oil/water partition coefficient of PNS

Solubility test of PNS: Excess PNS was added to glutathione bicarbonate Ringer solution (GBR), simulated tear fluid (STF), phosphate buffer USP (pH 6.8), and ultrapure water. The mixture was then maintained at (35 ± 0.5)°C and stirred using a magnetic stirrer (SCZL-4B, Henan, China) at 300 rpm for 24 h, while ensuring that excess PNS always remained. The collected samples were filtered with a 0.45 μm micropore filter, and the filtrate was diluted with GBR, STF, phosphate buffer USP (pH 6.8), and ultrapure water after 24 h. Finally, high performance liquid chromatography (HPLC) (Agilent 1260 HPLC, USA) was performed using 20 μL of the sample solution.

Stability test of PNS: PNS was added to GBR, STF, phosphate buffer USP (pH 6.8), and ultrapure water. The mixture was then maintained at (35 ± 0.5)°C and stirred using a magnetic stirrer (SCZL-4B) at 300 rpm. Samples were withdrawn at 0, 2, 4, 6, 8, and 10 h. The collected samples were filtered with a 0.45 μm micropore filter, and the filtrate was diluted with GBR, STF, phosphate buffer USP (pH 6.8), and ultrapure water. Then, 20 μL of sample solution was determined by HPLC (Agilent 1260 HPLC).

Exploiting the apparent oil/water partition coefficient of PNS[31], GBR, STF, PBS (pH 6.8), water, and octanol were mixed in equal amounts and placed in a conical flask, stirred at room temperature for 24 h, and allowed to stand overnight. After phase separation, octanol saturated with water (upper layer) was obtained as the oil phase, and water-saturated with octanol (lower layer) was obtained as the aqueous phase. Then, 25.42 mg PNS was accurately weighed and placed in a 25mL flask, diluted to scale in an aqueous phase to obtain an aqueous solution of PNS, and the initial concentration was determined. Then, 5 mL of the drug-containing solution was transferred to a bottle and the oil phase (octanol saturated with water) was added to make the water–oil ratio 1:1. This mixture was then continuously stirred at a constant temperature (35°C, 120 rpm) in the water bath for 12 h, and was then allowed to stand for 30 min. This allowed the separation of the two phases (oil and water). The lower aqueous phase was collected and centrifuged at 4,000 rpm for 10 min. The concentrations of ginsenoside Rg_1, ginsenoside Rb_1, and notoginsenoside R_1 in the water layer were determined by HPLC (Agilent 1260 HPLC), and the mean values were calculated. The apparent oil/water partition coefficient was calculated using the following formula:

$$P_{app} = \frac{(C_1 - C_2)}{C_2}$$

where C_1 is the concentration of the original drug in the aqueous phase and C_2 is the concentration of the drug in the equalized aqueous phase.

2.3 Preparation of in situ gelling system

Briefly, 0.5% (w/v) PNS and 0.05% (w/v) EDTA-2Na were dissolved in a certain amount of ultrapure water,

dispersed evenly in an ultrasonic cleaner (C3860A, Tianjin, China) and heated to 70°C with magnetic stirring. Then, HPMC was slowly added to the PNS solution under continuous magnetic stirring (SCZL-4B, Henan, China) for 2 min. After mixing, the solution was stirred again at room temperature until it was clarified. In addition, the accurately weighed Carbomer® 940 was slowly added into a certain volume of ultrapure water under high-speed agitation to make the dispersion uniform and was then stored in a refrigerator at 4°C for more than 12 h until the polymer was completely dissolved, giving a clear solution. The above two solutions were then stirred and evenly mixed. The gelling system was adjusted to pH 5.2 with 1 mol/L sodium hydroxide solution to yield the final pH-triggered *in situ* gelling systems.

2.4 Drug analysis

The quantitative determination of ginsenoside Rg_1, ginsenoside Rb_1, and notoginsenoside R_1 were carried out using HPLC (SPD-10A plus; Shimadzu Company, Japan). An Agilent Zorbax SB-C_{18} column (4.6 mm × 250 mm, 5 μm) was used with the column temperature maintained at 30°C. The flow rate was 1 mL/min, and the injection volume was 20 μL. The detection wavelength was set at 203 nm, and the mobile phase was water (A) and acetonitrile (B). The HPLC gradient program was set as follows: 25% → 25% B, 0–8 min; 25% → 50% B, 8–27 min; 50% → 50% B, 27–31min; 55% → 25% B, 31–36 min; 25% → 25% B, 36–40 min.

2.5 Formula optimization and drug release studies

2.5.1 Gelling capacity studies

Gelling systems comprising Carbopol® 940 and HPMC at various concentrations were prepared and their gelling capacity was evaluated to determine the compositions suitable for use as an *in situ* gelling systems[32]. The gelling capacity was measured by placing 1 mL of the *in situ* gelling system in a vial containing 2 mL STF and equilibrating at (35 ± 0.5)°C. The gel formation, gelation time, and the time required for the formed gel to dissolve were monitored visually and recorded.

2.5.2 In vitro drug release studies

An *in vitro* drug release test was performed using a membraneless dissolution model with a dissolution testing apparatus (ZRS-8G, Tianjin, China) to study the drug release behavior of PNS from the *in situ* pH-triggered gelling systems[33]. Gelling system (3 g) of different concentrations was transferred in triplicate into vials (1.24 cm inner diameter, and 3.83 cm deep), each of which was immersed in 200 mL STF, used as a release medium. Care was taken to prevent the breakdown of the gelling system and to ensure that there were no bubbles in the gel. The temperature and stirring rate were kept at (35 ± 1)°C and 100 rpm. At each time point, 2 mL aliquots were taken from the release medium and replaced with an equal volume of the release medium. The drug release of PNS was evaluated using HPLC (Shimadzu LC 10-AT, Japan). In addition, we used DDSolver 1.0 processing software to fit the release equation of the *in vitro* release data of the formulation A_3–B_2[34].

2.6 In vitro evaluation of the PNS-containing gel formulations

2.6.1 Rheological studies

The rheological properties were measured using the small sample adaptor of a rheometer (Brookfield DV-III, USA)[35]. The pH of the formulation A_3–B_2 was adjusted to pH 4.8, 5.0, 5.2, 5.8, 6.4, 7.0, or 7.4 with sodium hydroxide, respectively, and then the viscosity of the gel at different pH values was measured at room temperature to obtain the viscosity curve of the ophthalmic gel viscosity versus pH value.

The viscosity of different gelling systems [0.4% (w/v) HPMC E4M, 0.4% (w/v) Carbomer® 940, and 0.4% Carbomer® 940 – 0.4% HPMC E4M solution] were measured under non-physiological conditions [(25 ± 1)°C, pH 5.0] and physiological conditions [(35 ± 1)°C, pH 7.4]. The temperature was kept within ±1°C using circulating water (Wisdom) connected to the sample adaptor of the rheometer. Triethanolamine was added to the solution to raise the pH value of the sample to 7.4. Before each measurement, the samples were equilibrated on the plate for 5 min to reach the operating temperature. A typical operation involved changing the shear rate from 0 to 100 s^{-1} at a controlled ramp speed, holding for 0.1 min at 100 s^{-1}, and then reducing the shear rate to 0 s^{-1} at the same controlled ramp speed. Measurements were taken in triplicate.

A rheological study of formulation A_3–B_2 with PNS and no PNS under non-physiological conditions (25 ± 1°C, pH 5.0) and physiological condition (35 ± 1°C, pH 7.4) was conducted to investigate whether PNS would affect the rheological behavior of the gels.

2.6.2 Corneal permeation study

In vitro permeation profiles of the newly developed formulation A_3–B_2 were evaluated using isolated rabbit corneas[36]. In brief, preheated 35°C formulations 0.5 mL were placed on the cornea of the donor cell, with the epithelial surface facing the donor cell and the GBR in the receptor cell. At fixed time points (40, 80, 120, 160, 200, and 240 min), the receptor samples were completely removed from the receptor cell and replaced with an equal volume of fresh GBR. The samples were analyzed using ultra performance liquid chromatography (UPLC)–MS/MS and each formulation were analyzed six times.

The chromatographic separation of the analytes was carried out on an Acquity UPLC HSS T3 C_{18} column (50 mm × 2.1 mm, 1.8 μm, Waters, CA, USA) with the column temperature maintained at 40°C. A mobile phase consisting of water (A) and acetonitrile (B) was used for chromatographic separation by gradient elution. The UPLC gradient program was set as follows: 18% → 18% B, 0–7 min; 18% → 40% B, 7–13 min; 40% → 18% B, 13–14 min; and 18% → 18% B, 14–15 min. A highly efficient and symmetrical peak was obtained at a flow rate of 0.3 mL/min. The prepared 10 μL sample was injected into the chromatographic system, and the temperature of the autosampler was maintained at 4°C. The analyte was detected using electrospray positive ionization (ESI^+) in multiple reaction monitoring mode. The characteristic precursors $[M+Na]^+$ to product ions transitions for quantification were *m/z* 823.48 → 643.3 and *m/z* 955.52 → 775.3 for ginsenoside Rg_1 and notoginsenoside R_1, respectively. The ESI configuration was: gas temperature 350°C; gas flow rate 11 L/min; nebulizer 20 psi; capillary 4,000 V. The fragmentor was optimized at 280 and 300 V and the collision energy was 42 and 50 eV for ginsenoside Rg_1 and notoginsenoside R_1, respectively. The acquired data were processed using MassHunter analysis for QQQ (Version 4.1, Agilent, USA). The drug permeability was measured using apparent permeability

coefficient (P_{app}) and steady-state flux (J_{ss}) as follows:

$$p_{app} = \frac{\Delta Q}{\Delta t \cdot C_o \cdot A \cdot 60}$$

$$J_{ss} = C_0 \cdot P_{app}$$

where C_0 is the original concentration of the drug in the donor chamber, the $\Delta Q/\Delta t$ is the slope of the linear part of the cumulative permeated amount versus time plot, A is the penetrating region area (0.50 cm^2) and 60 is the factor for conversion of minute to second.

2.6.3 Accelerated stability studies

The selected formulation A_3–B_2 was stored for 6 months under accelerated test conditions [(30 ± 2)°C, RH (65 ± 5)%]. Periodic drug content (HPLC) assessment of the formulations was performed.

2.7 In vivo evaluation of the formulations

2.7.1 Ocular irritation study

Ocular irritation studies were carried out based on the Draize technique[37]. We evaluated the ocular tolerance of 6 New Zealand white rabbits without gross ocular defects. The formulations (100 μL) were instilled into the conjunctival sac of the left eye, 4 times a day, for 7 consecutive days. Normal saline was used as a control for the right eye. The injury of the eyes was evaluated, and the irritation to the cornea, conjunctiva, and iris were rated based on the Draize irritancy scale[37].

After examination, the animals were euthanized and their eyes were fixed with 4% paraformaldehyde. The tissue blocks were then washed, dehydrated, and embedded in Paraffin. Sagittal sections of 5 μm thickness were obtained and stained with hematoxylin and eosin (H&E). A pathological microscope (Olympus, Tokyo, Japan) was used to observe the presence of pathological changes in the tissue sections, in at least three randomly selected fields.

2.7.2 Preliminary pharmacokinetic study in the vitreous

Ginsenoside Rg_1 and notoginsenoside R_1 in dialysate samples were evaluated using UPLC–MS/MS system. UPLC–MS/MS determination method was the same as that described in "2.6.2. Corneal Penetration Study." The specificity, linearity, accuracy, precision, and stability of the system during storage and processing were established and verified.

The dialysate samples were centrifuged at 12,000 rpm for 10 min, and then 10 μL aliquots of the supernatants were injected into the UPLC–MS/MS system for analysis.

2.7.3 Microdialysis in vivo recovery

An *in vivo* microdialysis recovery experiment was conducted[38]. In a microdialysis experiment, there are usually two types of recoveries: *in vitro* recovery and *in vivo* recovery. In this study, we measured the *in vivo* recoveries of ginsenoside Rg_1 and notoginsenoside R_1 at a flow rate of 1.5 μL/min. In the constant temperature water bath (37 ± 0.5)°C with electromagnetic stirring, 50 mL of normal saline containing PNS was added to the beaker. The bent linear probe was inserted into the beaker and secured with tape to ensure that the effective dialysis window was completely immersed in the liquid. The pump flow rate was set to 1.5 μL/min, and serial solutions of the drugs in normal saline (10, 50, 125, 250, 500, and 1,000 ng/mL) were used as the infusion fluids. After 30 min of initial perfusion, samples were collected at an interval of 30 min. The results were calculated as the average of the readings from three replicates for each concentration.

2.7.4 Pharmacokinetic analysis

Before the experiments, the animals were kept in an environmentally controlled feeding room for 7 d. The ocular bioavailability of PNS in the vitreous of rabbit eyes was determined by microdialysis[38]. Linear microdialysis probes (Bioanalytical Systems, Inc. West Lafayette, IN, USA; 30 kDa MWCO; 320 μm outer diameter) were carefully implanted into the vitreous of right eyes of 12 rabbits (divided into two groups), which were anesthetized with a subcutaneous injection of lidocaine hydrochloride (about 0.75 mL/kg, judged by the absence of response of the eye to external stimuli). As dialysate, normal saline was infused by a microinjection pump (CMA 402, CMA Microdialysis AB, Kista, Stockholm, Sweden) at a flow rate of 1.5 μL/min through linear microdialysis probes. After the probe was implanted, the animals were stabilized for 12 h. One group of rabbits were intraocularly instilled with 41.67 μL/kg PNS ophthalmic gel (ginsenoside Rg_1 0.113 mg/kg and notoginsenoside R_1 0.033 mg/kg), and another group of rabbits were injected with Xueshuantong injection (PNS proportion; 14.00 mg/kg, that is ginsenoside Rg_1 7.736 mg/kg, and notoginsenoside R_1 3.521 mg/kg) by the ear vein. The dialysate samples were collected every 30 min for analysis during the first 6 h and every hour between 6 and 8 h. All dialysate samples were injected into the UPLC–MS/MS system for analysis.

2.8 Statistical analysis

The obtained data are expressed as mean ± SD. The experimental data were analyzed by SPSS 26.0. Analysis of variance and student *t* test were used to assess statistical significance. The differences were considered significant at $P < 0.05$ or $P < 0.01$.

3 Results and discussion

3.1 Testing the solubility, stability, and apparent oil/water partition coefficient of PNS

The solubilities of ginsenoside Rg_1, ginsenoside Rb_1, and notoginsenoside R_1 in GBR, STF, phosphate buffer USP (pH 6.8), and ultrapure water, which were maintained at (35 ± 0.5)°C, were shown in Table 1. According to the above results, ginsenoside Rg_1, ginsenoside Rb_1, and notoginsenoside R_1, the main components of PNS, were easily soluble in GBR, STF, phosphate buffer USP (pH 6.8), and ultrapure water; thus, the PNS sample used herein met the leakage conditions required for the *in vitro* release and corneal permeation studies.

The stabilities of ginsenoside Rg_1, ginsenoside Rb_1, and notoginsenoside R_1 in GBR, STF, phosphate buffer USP (pH 6.8), and ultrapure water, which were maintained at (35 ± 0.5)°C, are shown in Tables 2–4. The relative standard deviation (RSD) value of the peak area was less than 1%, indicating that the stabilities of these components were high.

As can be seen from Table 5, the log*P* values of ginsenoside Rg_1, ginsenoside Rb_1, and notoginsenoside R_1

Table 1

Solubility of PNS in different media at (35±0.5)°C (n=3).

Media	Ginsenoside Rg_1		Ginsenoside Rb_1		Notoginsenoside R_1	
	Mean±SD (mg/mL)	RSD (%)	Mean±SD (mg/mL)	RSD (%)	Mean±SD (mg/mL)	RSD (%)
GBR	264.93±0.08	0.03	90.29±0.69	0.76	77.88±0.08	0.10
STF	325.63±0.27	0.08	111.92±0.33	0.29	95.77±0.09	0.10
PBS 6.8	313.87±0.06	0.02	106.13±0.22	0.21	92.32±0.08	0.08
Ultrapure water	302.31±0.09	0.03	104.42±0.08	0.08	89.02±0.12	0.13

GBR: glutathione bicarbonate Ringer solution; PNS: *Panax notoginseng* saponins; RSD: relative standard deviation; STF: simulated tear fluid.

in different media were <1, indicating that these three components had strong hydrophilicity. The apparent oil/water partition coefficient of drugs is closely related to their permeability. Previously, it has been reported in the literature that the corneal stroma, which makes up 90% of the cornea, limits the transport and delivery of highly lipophilic drugs[39]. Paracellular spacing in the conjunctival tissue (230-fold higher than that in the cornea) also facilitates the passage of large hydrophilic molecules.

3.2 Formula optimization and drug release studies

3.2.1 Gelling capacity studies

Carbopol®940 was used as the excipient in the pH-triggered *in situ* gelling system. The aqueous solution turns into a stiff gel when its pH is raised[33,40]. However, the concentration of Carbopol®940 required to form stiff gels results in the formation of a highly acidic solution. This is not easily neutralized by the weak buffering effect of the tear fluid. The concentration of Carbopol®940 may be reduced by the addition of a viscosity-enhancing polymer, such as HPMC E4M, without affecting the gelling capacity and rheological properties of the delivery system[33].

The formulation should have an optimal viscosity to allow its easy instillation into the eye as a liquid and that would undergo a rapid sol-gel transition. In addition, the gel formed *in situ* should retain its integrity over a long time without dissolving or eroding. Gelling systems with different concentrations of Carbopol®940 and HPMC were prepared and their gelling capacities were evaluated to determine their optimal compositions required for suitable *in situ* gelling[33]. As shown in Table 6, grade "++" indicates a better gelling performance.

Table 2

Stability of ginsenoside Rg_1 in different media at (35±0.5)°C (n=3).

Media	Peak area						RSD (%)
	0h	2h	4h	6h	8h	10h	
GBR	2,944.67±1.74	2,936.30±3.00	2,928.73±1.31	2,925.83±1.25	2,923.30±1.45	2,921.87±0.80	0.29
STF	2,921.80±1.57	2,924.77±1.89	2,927.93±2.05	2,922.77±2.57	2,915.17±2.54	2,910.50±1.56	0.20
PBS 6.8	3,020.70±2.93	3,015.07±2.40	3,011.43±1.96	3,007.03±0.64	3,003.97±1.89	3,001.20±0.70	0.23
Ultrapure water	3,072.63±1.53	3,070.07±0.80	3,065.10±2.59	3,060.67±1.12	3,057.27±0.98	3,053.20±1.35	0.23

GBR: glutathione bicarbonate Ringer solution; RSD: relative standard deviation; STF: simulated tear fluid.

Table 3

Stability of ginsenoside Rb_1 in different media at (35±0.5)°C (n=3).

Media	Peak area						RSD (%)
	0h	2h	4h	6h	8h	10h	
GBR	922.70±1.13	919.07±0.83	917.23±0.96	915.70±0.10	914.77±0.68	912.80±0.35	0.36
STF	917.03±1.96	915.43±3.40	927.97±2.06	923.23±2.37	920.70±2.23	913.70±2.26	0.58
PBS 6.8	952.03±0.06	950.83±0.76	949.00±0.62	947.23±0.31	945.73±0.40	944.33±1.52	0.30
Ultrapure water	975.17±1.38	972.10±0.44	970.80±1.04	969.03±0.42	967.60±0.75	964.70±1.44	0.36

GBR: glutathione bicarbonate Ringer solution; RSD: relative standard deviation; STF: simulated tear fluid.

Table 4

Stability of notoginsenoside R1 in different media at (35±0.5)°C (n=3).

	Peak area						RSD (%)
	0h	2h	4h	6h	8h	10h	
GBR	669.63±0.72	666.80±0.53	665.40±0.44	664.33±0.57	664.13±0.55	664.93±1.17	0.30
STF	665.00±0.85	666.97±0.51	667.67±0.75	665.80±1.25	663.90±0.01	660.65±0.35	0.34
PBS 6.8	681.07±2.04	680.37±1.11	681.33±0.78	681.23±0.61	682.03±0.67	680.93±0.76	0.16
Ultrapure water	701.50±1.23	699.13±1.03	696.83±1.17	695.73±0.32	694.53±0.25	693.80±0.53	0.41

GBR: glutathione bicarbonate Ringer solution; RSD: relative standard deviation; STF: simulated tear fluid.

Table 5

Apparent oil/water partition coefficient of PNS (n = 3).

Media	Ginsenoside Rg_1		Ginsenoside Rb_1		Notoginsenoside R_1	
	P_{app}	log*P*	P_{app}	log*P*	P_{app}	log*P*
GBR	0.72 ± 0.01	−0.14 ± 0.01	0.23 ± 0.01	−0.65 ± 0.01	0.33 ± 0.01	−0.48 ± 0.01
STF	0.78 ± 0.01	−0.11 ± 0.01	0.26 ± 0.04	−0.60 ± 0.07	0.47 ± 0.04	−0.33 ± 0.03
PBS 6.8	0.76 ± 0.01	−0.12 ± 0.01	0.41 ± 0.01	−0.39 ± 0.01	0.38 ± 0.01	−0.42 ± 0.01
Ultrapure water	0.78 ± 0.01	−0.11 ± 0.01	0.44 ± 0.02	−0.36 ± 0.02	0.36 ± 0.01	−0.44 ± 0.01

GBR: glutathione bicarbonate Ringer solution; PNS: *Panax notoginseng* saponins; STF: simulated tear fluid.

3.2.2 *In vitro release*

The profiles of the cumulative amounts of PNS released for a variety of formulations of the *in situ* gelling system (A_1–B_4, A_1–B_5, A_2–B_3, A_2–B_4, and A_3–B_2) and PNS in STF (control solution) are shown in Figure 1. For the control solution, almost all ginsenoside Rg_1, ginsenoside Rb_1, and notoginsenoside R_1 were almost completely released immediately after the release test started. The PNS solution was released rapidly in STF; it was completely released in 15 min. In the case of the A_2–B_3 formulation, PNS was released completely within 2 h, while the A_2–B_4 and A_1–B_4 formulations showed longer PNS-release times (>3 h). The release of PNS from the A_1–B_5 formulation in prescription was low; among which, only 64.92% of notoginsenoside R_1 was released after 5 h. In case of the A_3–B_2 formulation, PNS was released completely in 3 h. This formulation exhibited a sustained PNS-release effect. Further, for this formulation, the release rates of ginsenoside Rg_1, ginsenoside Rb_1, and notoginsenoside R_1 reached more than 85%, which were close to the release rates observed in the case of the control solution group. These results indicated that the sustained PNS-release effect of the A_3–B_2 formulation was better than that of the other formulations and that this formulation could thus, be used as an ophthalmic drug delivery system for sustained PNS release.

Drug-release mechanisms can be represented *via* the following models: the zero-order, first-order, Peppas, Higuchi, and Weibull release models; among these, the Weibull model is widely used for fast release and slow drug-release fitting[41]. The results of the present study indicated that the release of ginsenoside Rg_1, ginsenoside Rb_1, and notoginsenoside R_1 in the PNS eye gel complied with the release equation of the Weibull model; these specific results were shown in Tables 7–9 and Figure 2.

3.3 *In vitro evaluation of formulations*

3.3.1 *Rheological studies*

The rheological behaviors of different gelling systems with pH values were studied. Figure 3A illustrated the viscosity change of formulation A_3–B_2 induced by pH. The gelation pH value of the polymer solution was pH 5.2. The viscosity suddenly increased after the pH reached 5.2, indicating the occurrence of sol–gel phase transition under these two conditions for the *in situ* gelling system.

Rheological behavior of different polymer solutions without PNS was studied[42]. Figure 3B showed the shear stress vs. shear rate flow curves of the HPMC E4M solution [0.4% (w/w)], Carbopol®940 solution [0.4% (w/w)], and formulation A_3–B_2 without PNS [0.4% Carbopol®940–0.4% HPMC E4M (w/v)] under non-physiological (pH 4.8 ± 0.1, 25°C) and physiological (pH 7.4 ± 0.1, 35°C) condition. For the HPMC E4M solution, the shear stress increased linearly with the increase of shear rate under non-physiological conditions, while the shear stress from physiological conditions to non-physiological conditions only slightly decreased. Under the two kinds of conditions, the HPMC E4M solution did not undergo a

Table 6

Formulations of PNS with different proportions of Carbopol®940 and HPMC and gelling capacity.

Formulations	Concentration (%, w/v)		Gelling capacity
	Carbopol®940 (A)	HPMC (B)	
A_1–B_1	0.2	0.2	+
A_1–B_2	0.2	0.4	+
A_1–B_3	0.2	0.6	+
A_1–B_4	0.2	0.8	++
A_1–B_5	0.2	1.0	++
A_2–B_1	0.3	0.2	+
A_2–B_2	0.3	0.4	+
A_2–B_3	0.3	0.6	++
A_2–B_4	0.3	0.8	++
A_2–B_5	0.3	1.0	+++
A_3–B_1	0.4	0.2	+
A_3–B_2	0.4	0.4	++
A_3–B_3	0.4	0.6	+++
A_3–B_4	0.4	0.8	+++
A_3–B_5	0.4	1.0	+++

+, gels after a few minutes (<10 min), dissolves rapidly; ++, gelation immediate, remains for few hours (10 min–3 h); +++, gelation immediate, remains for extended period (3–5 h).
PNS: Panax notoginseng saponins.

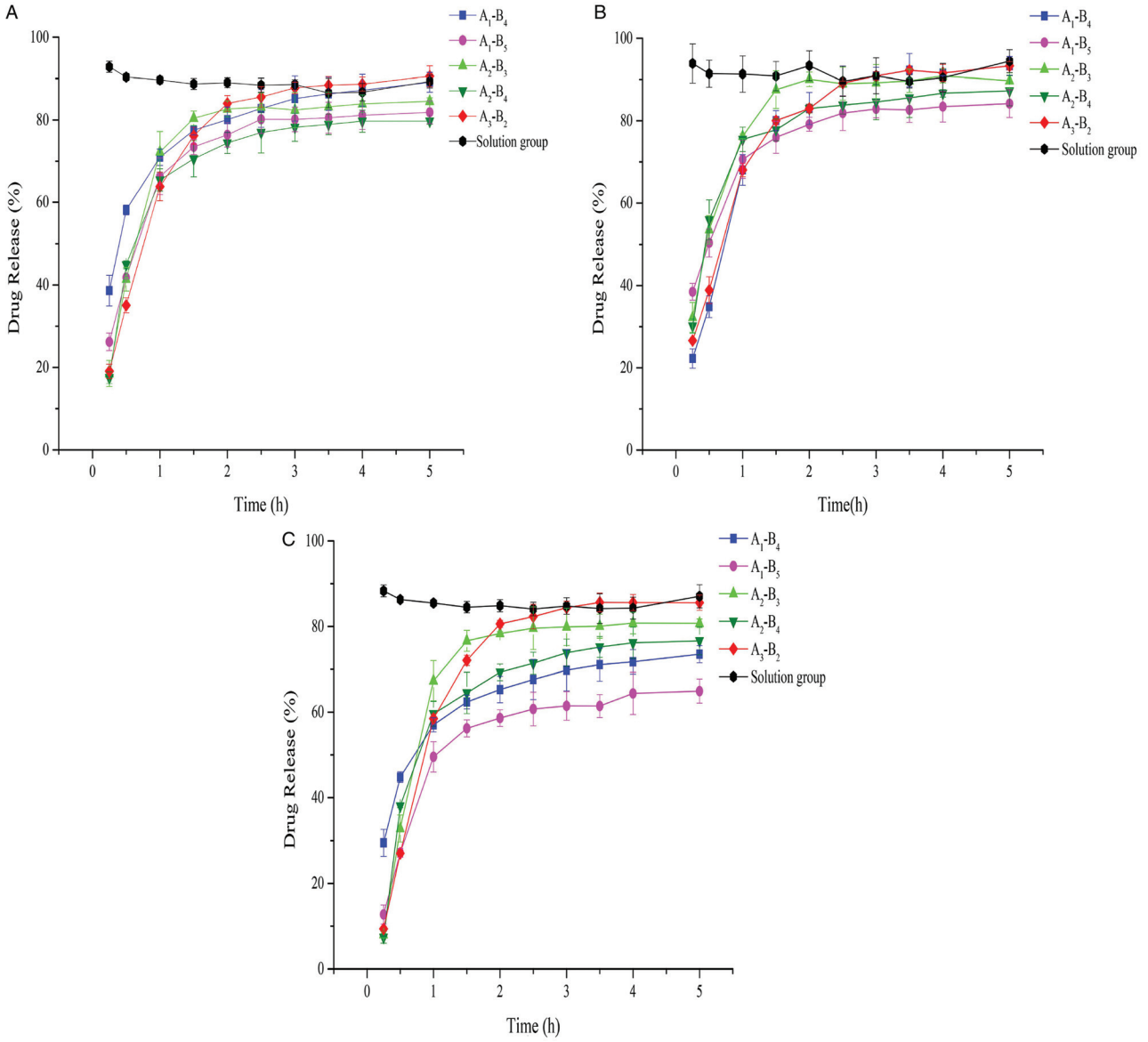

Figure 1. Study on the release of ginsenoside Rg_1, ginsenoside Rb_1, and notoginsenoside R_1 in different formulations (A) ginsenoside Rg_1, (B) ginsenoside Rb_1, and (C) notoginsenoside R_1.

phase change to turn into a gel but was still a free-flowing liquid, similar to pure water, exhibiting Newtonian-fluid flow behavior. In addition, for Carbopol® 940 solution and formulation A_3–B_2 without PNS under non-physiological conditions, and for the HPMC E4M solution under either non-physiological or physiological conditions, the shear stress increased linearly with the increase in shear rate, which also showed a Newtonian-flow behavior. Under physiological conditions, both solutions resisted the initial rotational movement, and the shear stress increased suddenly at higher shear rates. After the shear stress reached the yield point, the solutions began to flow. Therefore, the flow curves for these two solutions exhibited hysteretic pseudoplastic behavior under physiological conditions. At a shear rate of $100\,s^{-1}$, the shear stresses of Carbopol® 940 and formulation A_3–B_2 without

Table 7

Dissolution release equation fitting of ginsenoside Rg_1 in PNS ophthalmic gel.

Model name	Equation	*r*	AIC	MSC	MSE
Zero-order	$F_0 = 24.619 \times t$	0.8190	90.25	−0.37	755.63
First-order	$F = 100 \times [1 - \mathrm{Exp}(-0.710 \times t)]$	0.9871	57.63	2.88	28.96
Higuchi	$F = 46.607 \times t^{0.5}$	0.9080	73.40	1.31	140.13
Korsmeyer-Peppas	$F = 51.138 \times t^{0.412}$	0.9295	70.85	1.57	100.08
Hixson-Crowell	$F = 100 \times [1 - (1 - 0.196 \times t)^3]$	0.9841	66.04	2.05	67.16
Weibull	$F = 85.382 \times \{1 - \mathrm{Exp}[-((t-0.114)^{1.230})/0.777]\}$	0.9992	29.59	5.69	1.44

AIC: Akaike information criterion; MSC: mean square consistency; MSE: mean squared error; PNS: *Panax notoginseng* saponins.

Table 8

Dissolution release equation fitting of ginsenoside Rb1 in PNS ophthalmic gel.

Model name	Equation	*r*	AIC	MSC	MSE
Zero-order	$F_0 = 26.706 \times t$	0.8295	91.49	−0.60	855.28
First-order	$F = 100 \times [1 - \mathrm{Exp}(-t)]$	0.9940	54.34	3.11	20.84
Higuchi	$F = 51.051 \times t^{0.5}$	0.9152	74.10	1.13	150.31
Korsmeyer-Peppas	$F = 60.913 \times t^{0.331}$	0.9394	68.26	1.72	77.21
Hixson-Crowell	$F = 100 \times [1 - (1 - 0.259 \times t)^3]$	0.9910	64.82	2.06	59.40
Weibull	$F = 92.240 \times \{1 - \mathrm{Exp}[-((t + 0.113)^{1.204})/0.919]\}$	0.9973	41.38	4.41	4.69

AIC: Akaike information criterion; MSC: mean square consistency; MSE: mean squared error; PNS: *Panax notoginseng* saponins.

Table 9

Dissolution release equation fitting of notoginsenoside R1 in PNS ophthalmic gel.

Model name	Equation	*r*	AIC	MSC	MSE
Zero-order	$F_0 = 25.804 \times t$	0.8087	88.50	−0.03	634.54
First-order	$F = 100 \times [1 - \mathrm{Exp}(-0.863 \times t)]$	0.9724	62.82	2.54	48.66
Higuchi	$F = 49.159 \times t^{0.5}$	0.9009	73.76	1.45	145.27
Korsmeyer-Peppas	$F = 56.899 \times t^{0.361}$	0.9153	74.43	1.38	143.17
Hixson-Crowell	$F = 100 \times [1 - (1 - 0.235 \times t)^3]$	0.9651	68.87	1.93	89.13
Weibull	$F = 89.038 \times \{1 - \mathrm{Exp}[-((t + 0.015)^{1.227})/0.843]\}$	0.9996	24.88	6.33	0.90

AIC: Akaike information criterion; MSC: mean square consistency; MSE: mean squared error; PNS: *Panax notoginseng* saponins.

PNS under physiological conditions were about three to six times higher than the shear stresses under non-physiological conditions, indicating a significant sol–gel phase transition under these two conditions for two systems. The observed phase transitions of both solutions were mediated by a pH change from 5.0 to 7.4 which was attributable to the ionization of the Carbopol polymer. At pH 7.4, the mutual repulsion of ionized carboxyl groups may produce a more stretched Carbopol backbone, and these carboxyl groups may also form stable hydrogen

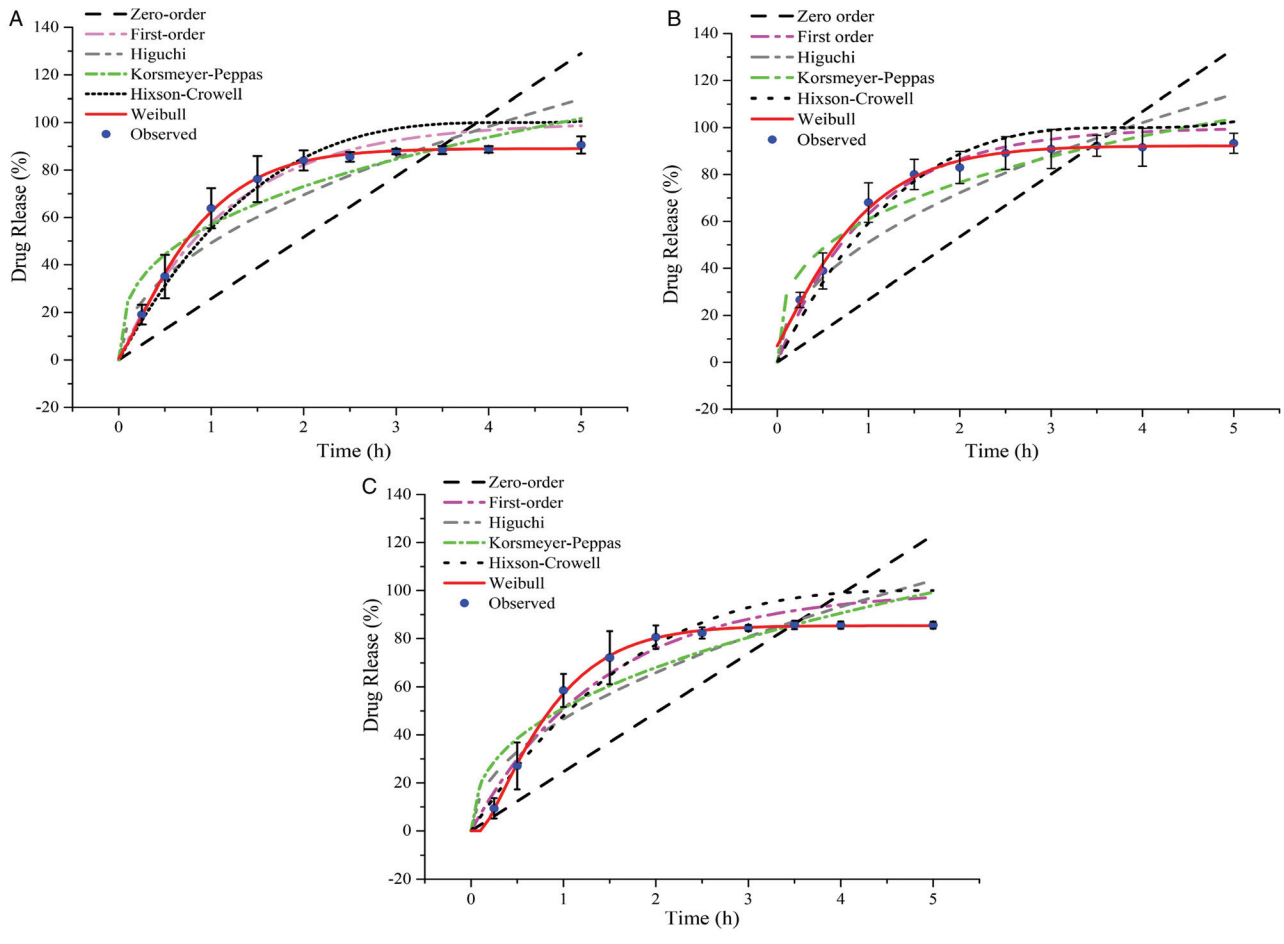

Figure 2. Model fitting curves of the release of ginsenoside Rg_1, ginsenoside Rb_1, and notoginsenoside R_1 (A) ginsenoside Rg_1, (B) ginsenoside Rb_1, and (C) notoginsenoside R_1.

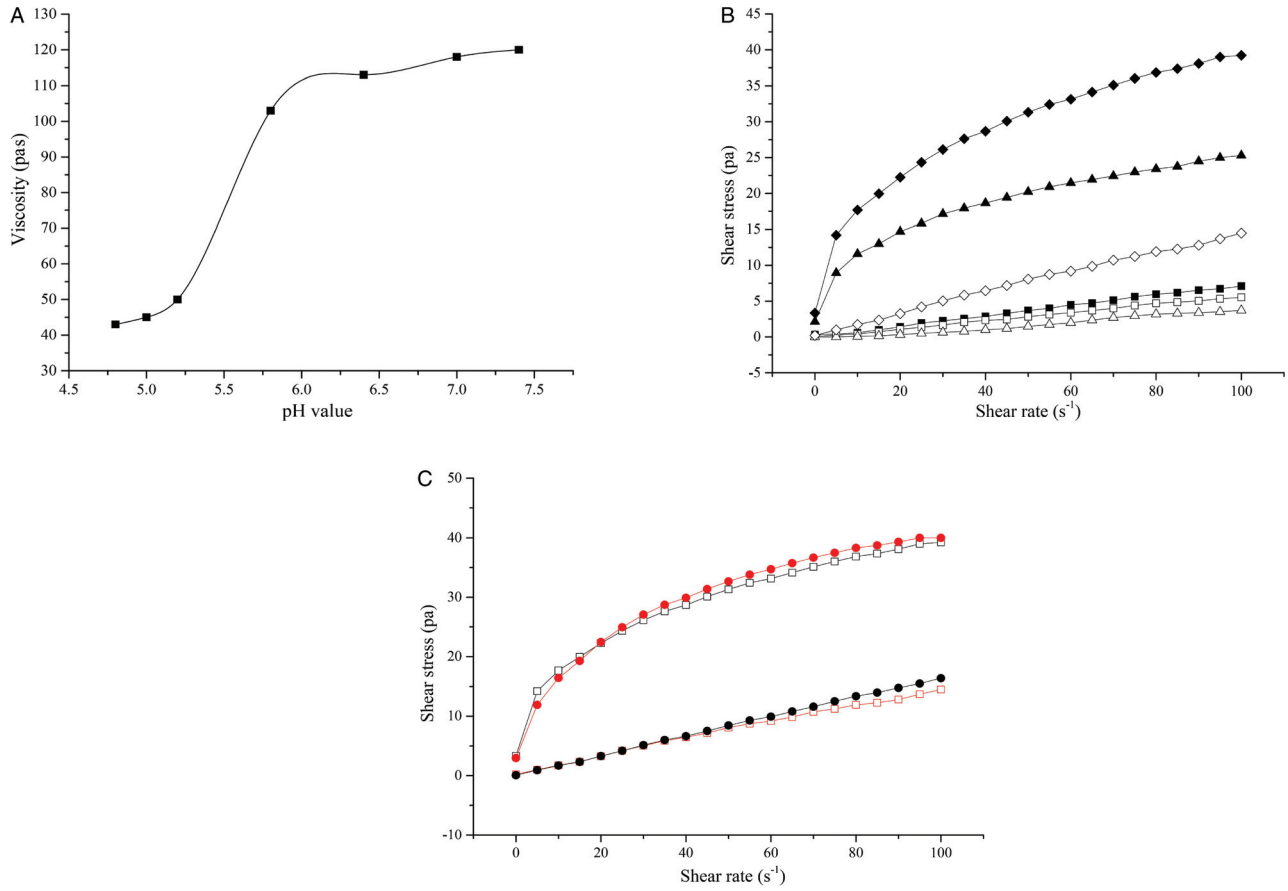

Figure 3. Rheological studies (formulation A_3–B_2). (A: pH-induced viscosity change of PNS in the *in situ* gelling system, B: shear stress vs. shear rate flow curves of different polymer solutions without PNS, ■: HPMC solution under physiological conditions; □: HPMC solution under non-physiological conditions; ▲: Carbopol®940 solution under physiological conditions; Δ: Carbopol®940 solution under non-physiological conditions; ◆: Formulation A_3–B_2 without PNS under physiological conditions; ◇: Formulation A_3–B_2 without PNS under non-physiological conditions, C: shear stress vs. shear rate flow curves of formulation A_3–B_2 with and without PNS, □: Formulation A_3–B_2 without PNS under physiological conditions; □: Formulation A_3–B_2 without PNS under non-physiological conditions; ●: Formulation A_3–B_2 with PNS under physiological conditions; ●: Formulation A_3–B_2 without PNS under non-physiological conditions.). HPMC: hydroxypropyl methylcellulose; PNS: *Panax notoginseng* saponins.

bonds with water molecules through hydrophilic interactions. The hydrophobicity of the Carbopol backbone may result in aggregation between hydrophobic chains. This cross-linking may lead to the formation of a more viscous gel at a pH of 7.4.

Rheological behaviors of formulation A_3–B_2 with and without PNS under non-physiological and physiological conditions were carried out to study the effects of PNS on the rheological behaviors of the formulation. As can be seen from Figure 3C, formulation A_3–B_2 with PNS was similar to that of A_3–B_2 formulation without PNS, indicating that the incorporation of PNS did not destroy the strong three-dimensional gel network formed under both non-physiological and physiological conditions[42].

3.3.2 Corneal permeation study

The cumulative penetration results of PNS ophthalmic gel on isolated rabbit corneas at different times were shown in Table 10 and Figure 4. The cumulative release of ginsenoside Rg_1 and notoginsenoside R_1 in 240 min were $(45.33 \pm 11.35)\ \mu g/mc^2$ and $(2.82 \pm 0.77)\ \mu g/mc^2$, respectively. *In vitro* corneal transmittance parameters of pH-sensitive PNS *in situ* gel are shown in Table 11. The release behavior of ginsenoside Rg_1 and notoginsenoside R_1 in cornea *in vitro* was still consistent with the Weibull model, which laid a foundation for subsequent preliminary *in vivo* evaluation. The specific results were shown in Tables 12 and 13 and Figure 5.

The low drug concentration in dialysate were determined using UPLC–MS/MS. However, while establishing the analytical method for evaluating corneal permeability *in vitro*, our mass spectrometry results showed that ginsenoside Rb_1 was extremely unstable in an aqueous solution. This could be attributed to the following reasons: 1) the ionization degree of saponins is closely related to its molecular formula. Thus, the greater the molecular polarity, the easier it is to ionize it in the ESI ion source

Table 10

Cumulative transmission volume per unit area of rabbit cornea of PNS ophthalmic gel (n = 6).

	$Q/(\mu g/mc^2)$	
Time (min)	Ginsenoside Rg_1	Notoginsenoside R_1
40	0.65 ± 0.69	0.07 ± 0.04
80	4.90 ± 3.97	0.41 ± 0.18
120	13.07 ± 6.33	0.90 ± 0.59
160	23.04 ± 7.95	1.51 ± 0.65
200	34.84 ± 10.31	2.39 ± 0.70
240	45.33 ± 11.35	2.82 ± 0.77

PNS: *Panax notoginseng* saponins.

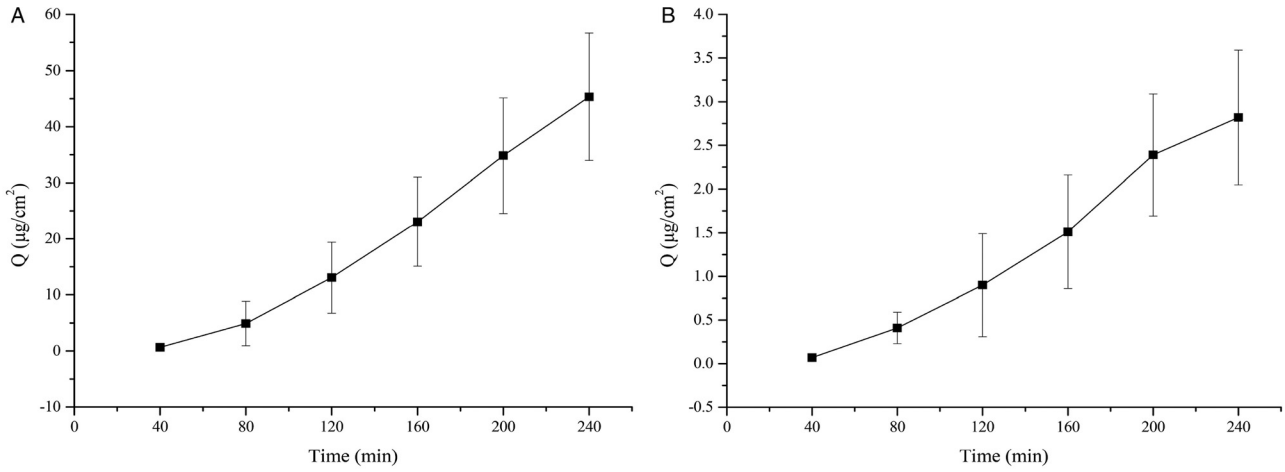

Figure 4. *In vitro* corneal transmittance curves of ginsenoside Rg_1 and notoginsenoside R_1 ($n=6$) (A) ginsenoside Rg_1 and (B) notoginsenoside R_1.

and obtain a stronger mass spectrum signal. Ginsenoside Rb_1 was the least polar among the three components, which made it difficult to ionize[43]. 2) Under the positive ion mode detection, saponin molecules occur as adducts of sodium ion $[M+Na]^+$ for the base peak; the sodium ion adducts exhibit instability, possibly due to the sodium source. In addition, saponins have high ion abundance and show a low signal-to-noise ratio in positive ion mode. Compared with ginsenoside Rg_1 and notoginsenoside R_1, ginsenoside Rb_1 is more obvious[44]. Therefore, for evaluating corneal permeability *in vitro*, we established an analytical method to determine only ginsenoside Rg_1 and notoginsenoside R_1. In future studies, we will try different sample pretreatment methods to optimize liquid quality to solve this problem.

3.3.3 Stability evaluation

Accelerated stability studies of formulation A_3–B_2 were evaluated. Table 14 showed that the RSD value of the drug content for A_3–B_2 was less than 2%.

Table 11

***In vitro* corneal transmittance parameters of PNS ophthalmic gel.**

Compounds	$Q-t$ regression equation	r	$P_{app} \times 10^4$ (cm/s)	J_{ss} (μg/cm²/s)
Ginsenoside Rg_1	$Q=230.83t-12{,}008$	0.9905	34.16 ± 7.91	7.69 ± 1.78
Notoginsenoside R_1	$Q=580.91t-683.53$	0.9913	7.92 ± 2.25	0.48 ± 0.14

PNS: *Panax notoginseng* saponins.

Table 12

***In vitro* corneal release equation fitting of ginsenoside Rg1 in PNS ophthalmic gel.**

Model name	Equation	r	AIC	MSC	MSE
Zero-order	$F_0=0.162 \times t$	0.9905	33.64	1.72	39.03
First-order	$F=100 \times [1-\text{Exp}(-0.002 \times t)]$	0.9819	35.77	1.36	55.67
Higuchi	$F=1.997 \times t^{0.5}$	0.9661	40.81	0.53	128.88
Korsmeyer-Peppas	$F=0.002 \times t^{1.809}$	0.9980	16.02	4.66	1.85
Hixson-Crowell	$F=100 \times [1-(1-0.196 \times t)^3]$	0.9849	35.14	1.47	50.11
Weibull	$F=64.268 \times \{1-\text{Exp}[-((t-0.114)^{2.466})/606112.836]\}$	0.9999	−2.22	7.70	0.08

AIC: Akaike information criterion; MSC: mean square consistency; MSE: mean squared error; PNS: *Panax notoginseng* saponins.

Table 13

***In vitro* corneal release equation fitting of notoginsenoside R_1 in PNS *in situ* gel.**

Model name	Equation	r	AIC	MSC	MSE
Zero-order	$F_0=0.011 \times t$	0.9913	−0.65	1.90	0.13
First-order	$F=100 \times [1-\text{Exp}(-0.0001 \times t)]$	0.9910	−0.50	1.88	0.13
Higuchi	$F=0.132 \times t^{0.5}$	0.9710	7.22	0.59	0.48
Korsmeyer-Peppas	$F=0.0003 \times t^{1.656}$	0.9945	−11.85	3.77	0.02
Hixson-Crowell	$F=100 \times [1-(1-0.00003 \times t)^3]$	0.9911	−0.55	1.88	0.13
Weibull	$F=89.038 \times \{1-\text{Exp}[-((t-34.988)^{1.283})/31261.363]\}$	0.9963	−12.67	3.91	0.01

AIC: Akaike information criterion; MSC: mean square consistency; MSE: mean squared error; PNS: *Panax notoginseng* saponins.

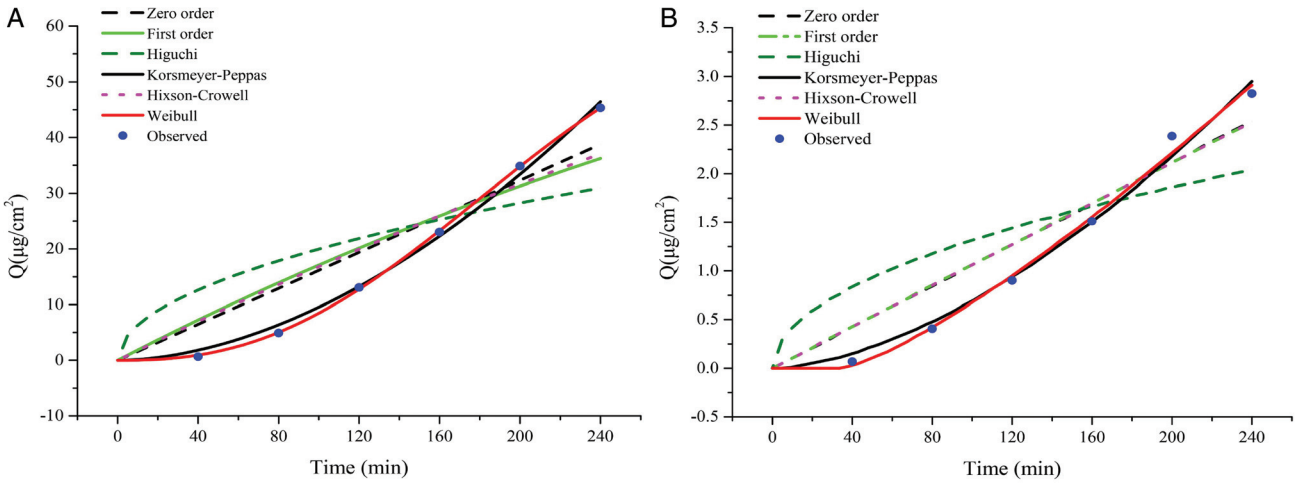

Figure 5. Model fitting curves of the release behavior of ginsenoside Rg_1 and notoginsenoside R_1 in PNS ophthalmic gel through the cornea *in vitro* (A) ginsenoside Rg_1 and (B) notoginsenoside R_1. PNS: *Panax notoginseng* saponins.

3.4 In vivo evaluation of formulations

3.4.1 Ocular irritation study

In all observations, the scores for the gels and control solution, as per the Draize irritancy scale, were 0[45]. No obvious damage to the cornea, conjunctiva, or iris were observed. This indicated that the gel did not irritate the ocular tissues, and therefore, was safe for ocular treatment. The histological examination of rabbit eyes (cornea, conjunctiva, and iris) are shown in Figure 6. The results showed normal and healthy ocular tissues and structures in each group. Moreover, the results of the histological examination in the gel and control groups were comparable.

3.4.2 Preliminary pharmacokinetic analysis in the vitreous

The typical chromatograms of blank dialysate, dialysate mixed with 125.00 ng/mL stock solutions of ginsenoside Rg_1 and notoginsenoside R_1, and dialysate samples showed no endogenous interference in the retention time of analytes, demonstrating the specificity of analysis. The retention time of ginsenoside Rg_1 and notoginsenoside R_1 was 7.83 and 5.97 min, respectively. The calibration curves were generated in the range of 1–250 ng/mL and the goodness of fit (r) was greater than 0.997. The intra- and inter-day imprecisions were lower than 2.87% and 2.55%, respectively, and the accuracy in the dialysate was within ±3.25%, indicating the overall good reproducibility of the method. All analytes present in the dialysate samples were stable when stored for 15 h at room temperature and for 12 h in the autosampler at 4°C. The stability met the conventional pharmacokinetic requirements. Further details were provided in the supplementary material, http://links.lww.com/AHM/A5.

The linear equation was drawn from (C_d–C_p) versus C_p (C_d, drug concentration in dialysate; C_p, drug concentration in the infusion fluid), and the recovery was given by the slope of the line[38]. The zero-abscissa assumed that the corresponding concentration around the probe compound in the solution was consistent with the actual concentration. Figure 7 showed the linear regression between (C_d–C_p) and C_p. The equation and recovery were illustrated in Table 15.

The concentration-time curves in rabbit eyes of PNS *in situ* gel *via* ocular administration and Xueshuantong solution for injection after intravenous administration were illustrated in Figure 8. The calculated pharmacokinetic parameters were shown in Table 16. The C_{max} of ginsenoside Rg_1 and notoginsenoside R_1 was (75.69 ± 19.94) and (16.92 ± 6.48) ng/mL, respectively, after being instilled into the PNS *in situ* gel *via* ocular administration in rabbits. The C_{max} of ginsenoside Rg_1 and notoginsenoside R_1 after intravenous administration of Xueshuantong solution for injection by ear vein was (40.09 ± 15.59) and (9.70 ± 2.75) ng/mL, respectively. The C_{max} of ginsenoside Rg_1 and notoginsenoside R_1 in the PNS gel administration group was 1.89 times and 1.74 times that of the Xueshuantong injection group, respectively. The bioavailability of ginsenoside Rg_1 and notoginsenoside R_1 in the PNS gel group were 6,322.35% ± 2,723.59% and 8,167.25% ± 1,342.50%, respectively. PNS ophthalmic

Table 14

Accelerated stability results of PNS ophthalmic gel (n = 3).

	Ginsenoside Rg_1 (mg/mL)			Ginsenoside Rb_1 (mg/mL)			Notoginsenoside R_1 (mg/mL)		
Month	1	2	3	1	2	3	1	2	3
0	2.24	2.36	2.37	0.95	1.09	1.09	0.59	0.61	0.61
1	2.23	2.36	2.29	0.95	1.10	1.06	0.60	0.61	0.59
2	2.24	2.36	2.30	0.95	1.09	1.07	0.59	0.61	0.59
3	2.24	2.38	2.29	0.95	1.09	1.07	0.60	0.61	0.59
6	2.24	2.37	2.30	0.94	1.09	1.06	0.59	0.61	0.59
RSD (%)	0.21	0.24	1.30	0.25	0.16	0.01	0.60	0.00	1.26

PNS: *Panax notoginseng* saponins; RSD: relative standard deviation.

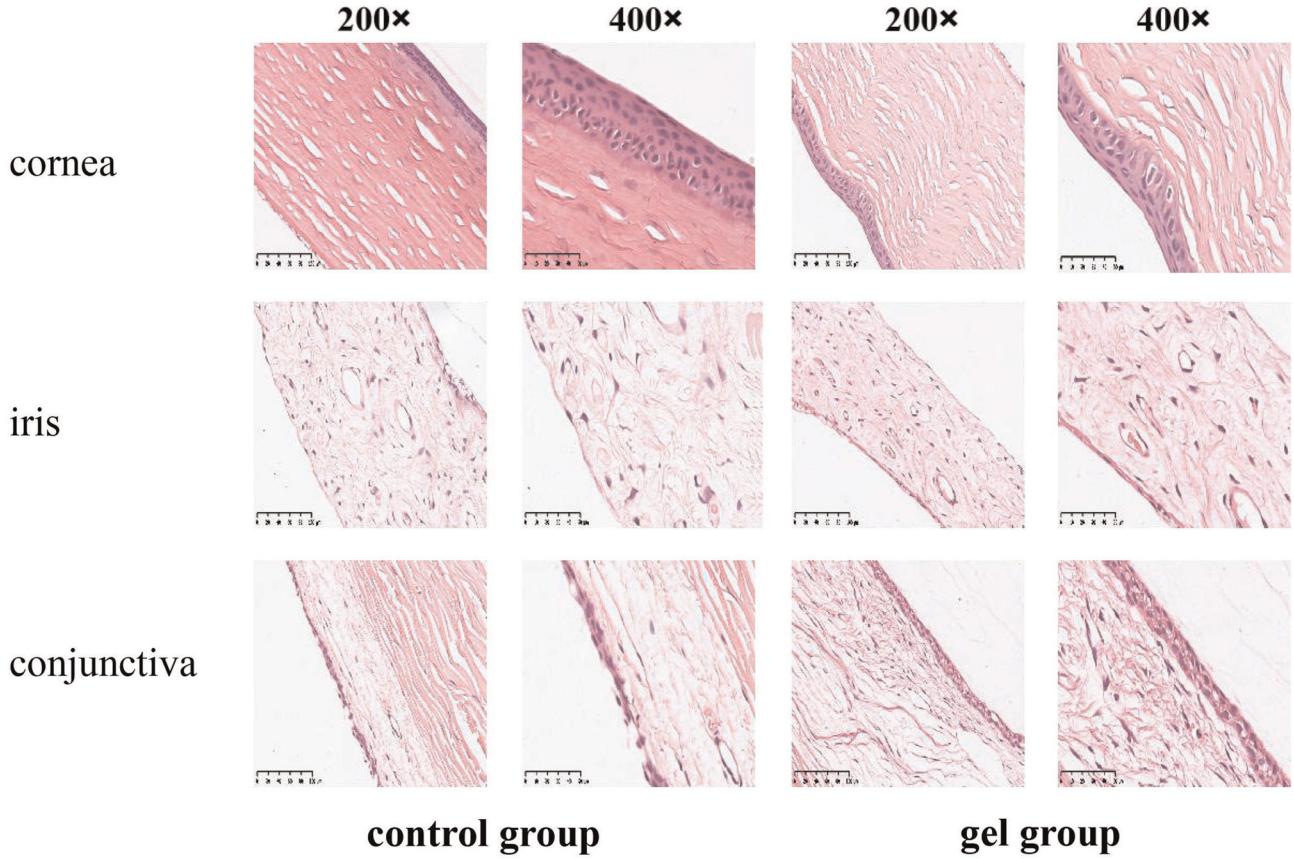

Figure 6. Pathological results of rabbit eye irritation test.

in situ gel greatly improves the ocular bioavailability of drugs. *In vivo* results further demonstrated that the *in situ* gelling system has the ability to maintain drug release, making it an ideal ocular delivery system for improving ocular bioavailability.

Nevertheless, there are some shortcomings in this pharmacokinetic test. Owing to the limitation of the dosage of PNS *in situ* gel, only about 100 μL can be given to rabbits. The dose of Xueshuantong (listed on the market) injection group was calculated based on the human clinical therapeutic dose. This led to a large difference in the dosage of the two groups. In the follow-up study, we will increase the drug content of the PNS in the *in situ* gel as much as possible and adjust the dose of the Xueshuantong injection group to make it close to the PNS *in situ* gel group. As far as possible, pharmacokinetic tests should be carried out when the doses of the two administration groups are the same to highlight the superiority of *in situ* gel for ocular administration. In addition, similar problems were observed with the

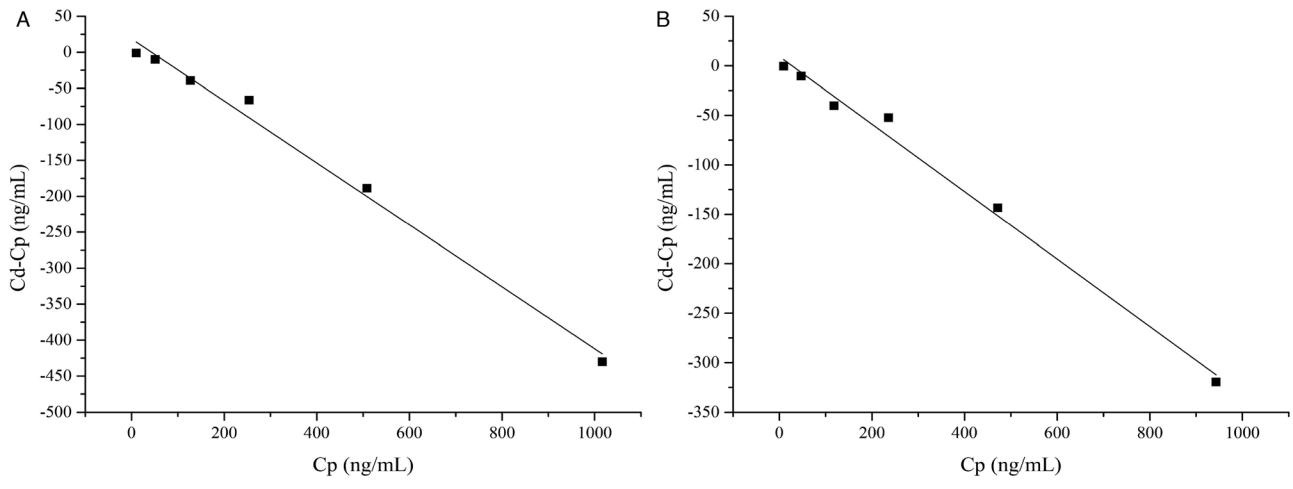

Figure 7. Recovery of *in vivo* microdialysis (A) ginsenoside Rg_1 and (B) notoginsenoside R_1.

Table 15

Recovery of *in vivo* microdialysis.

Compounds	Linear equation	*r*	Recovery (%)
Ginsenoside Rg_1	$y=-0.4305x+18.524$	−0.9958	43.05 ± 0.22
Notoginsenoside R_1	$y=-0.3411x+9.3$	−0.9958	34.11 ± 1.15

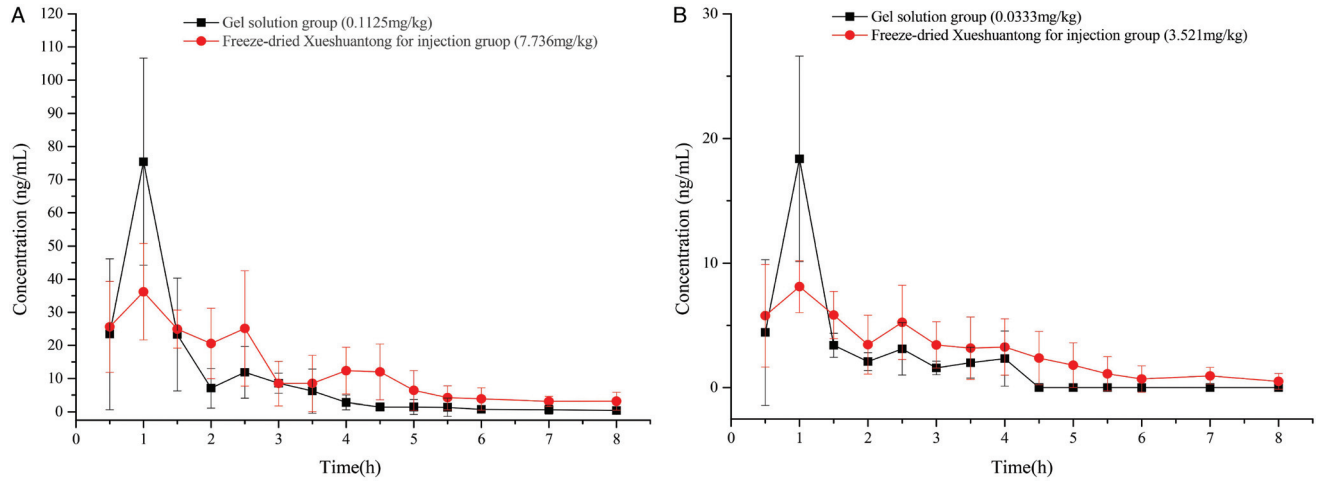

Figure 8. Drug concentration-time curve of ginsenoside Rg_1 and notoginsenoside R_1 in rabbit eye microdialysate (A) ginsenoside Rg_1 and (B) notoginsenoside R_1.

determination method of the corneal part *in vitro*. We established an analytical method to determine only ginsenoside Rg_1 and notoginsenoside R_1[43–44]. In future studies, we will try different methods to solve this problem.

4 Conclusions

In this study, we used Carbopol®940, a commonly used pH-sensitive polymer and a thickener HPMC E4M as a gel matrix to prepare an ophthalmic *in situ* gel of PNS. *In vivo* results further demonstrated that the *in situ* gelling system is capable of sustained drug release, making it an ideal ocular delivery system for improving posterior ocular bioavailability of medications. This article lays the foundation for the research of the delivery of PNS *via* pH-sensitive *in situ* gels and the development and improvement of related preparations and simultaneously, it combines TCM with a cutting edge *in situ* gel preparation method to provide new avenues for the treatment of posterior ocular diseases such as DR.

Conflict of interest statement

The authors declare no conflict of interest.

Funding

None specific to this article.

Table 16

Pharmacokinetic parameters of ginsenoside Rg_1 and notoginsenoside R_1 after administration of PNS gel and freeze dried Xueshuantong for injection (n = 6).

Parameters	PNS gel solution group		Freeze-dried Xueshuantong for injection group	
	Ginsenoside Rg_1	Notoginsenoside R_1	Ginsenoside Rg_1	Notoginsenoside R_1
C_{max} (ng/mL)	75.69 ± 19.94*	16.92 ± 6.48*	40.09 ± 15.59	9.70 ± 2.75
T_{max} (h)	1.08 ± 0.19	0.92 ± 0.19	1.75 ± 0.75	1.17 ± 0.62
AUC_{0-8h} (ng·h/mL)	73.03 ± 16.27	12.65 ± 4.80	104.98 ± 49.08	23.90 ± 11.37
$AUC_{0-\infty}$ (ng·h/mL)	103.56 ± 54.29	18.75 ± 8.87	134.66 ± 86.02	31.69 ± 13.59
Lz (1/h)	0.83 ± 0.53	0.52 ± 0.16	0.35 ± 0.14	0.32 ± 0.18
$T_{1/2}$ (h)	3.42 ± 5.60	1.48 ± 0.58	2.45 ± 1.28	3.50 ± 2.70
Vz/F (mL/kg)	3,418.61 ± 3,734.63**	4,055.88 ± 884.67**	227,465.34 ± 71,027.15	658,792.04 ± 607,495.50
Cl/F (mL/h/kg)	1,292.72 ± 418.07**	2,133.82 ± 818.39**	82,859.26 ± 47,912.50	124,504.82 ± 31,794.10
MRT (h)	1.55 ± 0.24*	1.28 ± 0.26*	2.50 ± 0.62	2.51 ± 0.73

PNS gel solution group vs. freeze-dried Xueshuantong for injection group.
PNS: Panax notoginseng saponins.
* $P<0.05$. ** $P<0.01$.

Author contributions

Peng Lu, Yue Xing, Jiaxin Pi, and Zhidong Liu participated in the research design and writing of the paper. Yue Xing, Renxing Wang, Dereje Kebebe, Yanquan Gao, Qingqing Zhang, Bin Xing, Ying Zhang, Changxiang Yu, Xinfu Cai, and Qiang Shang participated in the performance of the research. Jiaxin Pi and Zhidong Liu contributed new reagents or analytic tools. Peng Lu and Yue Xing participated in data analysis.

Ethical approval for animal studies

The protocols and any amendments or procedures involved in the care or use of animals in the study were in compliance with the regulations for animal experimentation issued by the State Committee of Science and Technology of China and approved by TJUTCM's Institutional Animal Care and Use Committee (Document number TCM-LAEC2018031).

Acknowledgments

We acknowledge the help of Mr. Ebuka-Olisaemeka Nwafor, who kindly improved the language of the paper.

References

[1] Chen Z, Li C, Yang C, et al. Lipid regulation effects of raw and processed Notoginseng Radix Et Rhizome on steatotic Hepatocyte L02 Cell. *Biomed Res Int* 2016;8(11):1–9.
[2] Fan Y, Qiao Y, Huang J, et al. Protective effects of *Panax notoginseng* saponins against high glucose-induced oxidative injury in rat retinal capillary endothelial cells. *Evid Based Complement Alternat Med* 2016;2:1–9.
[3] Jin Z, Gao L, Zhang L, et al. Antimicrobial activity of saponins produced by two novel endophytic fungi from *Panax notoginseng*. *Nat Prod Res* 2017;31(22):2700–2703.
[4] Liao J, Wei B, Chen H, et al. Bioinformatics investigation of therapeutic mechanisms of Xuesaitong capsule treating ischemic cerebrovascular rat model with comparative transcriptome analysis. *Am J Transl Res* 2016;8(5):2438–2449.
[5] Ratno Budiarto B, Chan WH. Oxidative stresses-mediated apoptotic effects of ginsenoside Rb1 on pre- and post-implantation mouse embryos *in vitro* and *in vivo*. *Environ Toxicol* 2017;32 (8):1990–2003.
[6] Zhou P, Xie W, Meng X, et al. Notoginsenoside R1 ameliorates diabetic retinopathy through PINK1-dependent activation of mitophagy. *Cells* 2019;8(3):213.
[7] Jian W, Yu S, Tang M, et al. A combination of the main constituents of Fufang Xueshuantong capsules shows protective effects against streptozotocin-induced retinal lesions in rats. *J Ethnopharmacol* 2016;182:50–56.
[8] Li C, Xu T, Zhou P, et al. Post-marketing safety surveillance and re-evaluation of Xueshuantong injection. *BMC Compl Alternat* 2018;18(1):277.
[9] Xu C, Wang W, Wang B, et al. Analytical methods and biological activities of *Panax notoginseng* saponins: recent trends. *J Ethnopharmacol* 2019;236:443–465.
[10] Gu CZ, Lyu JJ, Zhang XX, et al. Triterpenoids with promoting effects on the differentiation of PC12 cells from the steamed roots of *Panax notoginseng*. *J Nat Prod* 2015;78(8):1829–1840.
[11] Liu MH, Yang BR, Cheung WF, et al. Transcriptome analysis of leaves, roots and flowers of *Panax notoginseng* identifies genes involved in ginsenoside and alkaloid biosynthesis. *BMC Genomics* 2015;16(1):265.
[12] Han S, Chen Y, Wang J, et al. Anti-thrombosis effects and mechanisms by Xueshuantongcapsule under different flow conditions. *Front Pharmacol* 2019;10:35.
[13] Wang FJ, Wang SX, Chai LJ, et al. Xueshuantong injection (lyophilized) combined with salvianolate lyophilized injection protects against focal cerebral ischemia/reperfusion injury in rats through attenuation of oxidative stress. *Acta Pharmacol Sin* 2018;39(6):998–1011.
[14] Huang Y, Guo B, Shi B, et al. Chinese herbal medicine Xueshuantong enhances cerebral blood flow and improves neural functions in Alzheimer's disease mice. *J Alzheimer's Dis* 2018;63 (3):1089–1107.
[15] Liu Z, Zhang Q, Ding L, et al. Preparation procedure and pharmacokinetic study of water-in-oil nanoemulsion of *Panax notoginseng* saponins for improving the oral bioavailability. *Curr Drug Deliv* 2016;13(4):600–610.
[16] Chen XN, Li DQ, Zhao MD, et al. Pharmacokinetics of *Panax notoginseng*, saponins in adhesive and normal preparation of Fufang Danshen. *Eur J Drug Metab Pharmacokinet* 2018;43 (2):215–225.
[17] Wu Y, Liu Y, Li X, et al. Research progress in *in situ* gelling ophthalmic drug delivery system. *Asian J Pharm Sci* 2019;14(1):1–15.
[18] Loftsson T, Stefánsson E. Cyclodextrins and topical drug delivery to the anterior and posterior segments of the eye. *Int J Pharmaceut* 2017;531(2):413–423.
[19] Kaarniranta K, Xu H, Kauppinen A. Mechanistical retinal drug targets and challenge. *Adv Drug Deliver Rev* 2018;126:177–184.
[20] Wong CW, Wong TT. Posterior segment drug delivery for the treatment of exudative age-related macular degeneration and diabetic macular oedema. *Br J Ophthalmol* 2019;103(10):1356–1360.
[21] Gough G, Szapacs M, Shah T, et al. Ocular distribution and pharmacokinetic study of a small 13 kDa domain antibody after intravitreal, subconjuctival and eye drop administration in rabbits. *Exp Eye Res* 2018;167:14–17.
[22] Makwana SB, Patel VA, Parmar SJ. Development and characterization of *in situ* gel for ophthalmic formulation containing ciprofloxacin hydrochloride. *Results Pharma Sci* 2015;6:1–6.
[23] Gote V, Sikder S, Sicotte J, et al. Ocular drug delivery: present innovations and future challenges. *J Pharmacol Exp Ther* 2019;370 (3):602–624.
[24] Ye T, Yuan K, Zhang W, et al. Prodrugs incorporated into nanotechnology-based drug delivery systems for possible improvement in bioavailability of ocular drugs delivery. *Asian J Pharm Sci* 2013;8(4):207–217.
[25] Shi H, Wang Y, Bao Z, et al. Thermosensitive glycol chitosan-based hydrogel as a topical ocular drug delivery system for enhanced ocular bioavailability. *Int J Pharmaceut* 2019;570:118688.
[26] Khattab A, Marzok S, Ibrahim M. Development of optimized mucoadhesive thermosensitive pluronic based *in situ* gel for controlled delivery of latanoprost: antiglaucoma efficacy and stability approaches. *J Drug Deliv Sci Tec* 2019;53:101134.
[27] Pang X, Li J, Pi J, et al. Increasing efficacy and reducing systemic absorption of brimonidine tartrate ophthalmic gels in rabbits. *Pharm Dev Technol* 2018;23(3):231–239.
[28] Zhang J, Xie Y, Zhou T, et al. Development of natamycin-hydroxypropyl-beta-cyclodextrin inclusion complex, ion-triggered *in situ* gel for sustained ocular delivery: *in vitro, ex vivo* evaluation and ocular pharmacokinetics study. *Invest Ophth Vis Sci* 2018;59 (9):2676.
[29] Fernández-Ferreiro A, Silva-Rodríguez J, Otero-Espinar FJ, et al. *In vivo* eye surface residence determination by high-resolution scintigraphy of a novel ion-sensitive hydrogel based on gellan gum and kappa-carrageenan. *Eur J Pharm Biopharm* 2017;114: 317–323.
[30] Duan Y, Cai X, Du H, et al. Novel *in situ* gel systems based on P123/TPGS mixed micelles and gellan gum for ophthalmic delivery of curcumin. *Colloids Surf B Biointerfaces* 2015;128:322–330.
[31] Wang H, Qin Y, Li B, et al. Biological modification of montan resin from lignite by *Bacillus benzoevorans*. *Appl Biochem Biotechnol* 2019;188(4):965–976.
[32] Ranch KM, Maulvi FA, Naik MJ, et al. Optimization of a novel *in situ* gel for sustained ocular drug delivery using Box-Behnken design: *in vitro, ex vivo, in vivo* and human studies. *Int J Pharm* 2019;554:264–275.
[33] Wu H, Liu Z, Peng J, et al. Baicalin-containing *in situ* pH-triggered gelling system for sustained ophthalmic drug delivery. *Int J Pharm* 2011;410(1–2):31–40.
[34] Öztürk AA, Namlı İ, Güleç K, et al. Diclofenac sodium loaded PLGA nanoparticles for inflammatory diseases with high anti-inflammatory properties at low dose: formulation, characterization and *in vivo* HET-CAM analysis. *Microvasc Res* 2020;130:103991.
[35] Ma Q, Luo R, Zhang H, et al. Design, characterization, and application of a pH-triggered *in situ* gel for ocular delivery of vinpocetine. *AAPS Pharm Sci Tech* 2020;21(7):253.

[36] Jain P, Jaiswal CP, Mirza MA, et al. Preparation of levofloxacin loaded *in situ* gel for sustained ocular delivery: *in vitro* and *ex vivo* evaluations. *Drug Dev Ind Pharm* 2020;46(1):50–56.
[37] Bin-Jumah M, Gilani SJ, Jahangir MA, et al. Clarithromycin-loaded ocular chitosan nanoparticle: formulation, optimization, characterization, ocular Irritation, and antimicrobial activity. *Int J Nanomedicine* 2020;15:7861–7875.
[38] Wang S, Li D, Pi J, et al. Pharmacokinetic and ocular microdialysis study of oral ginkgo biloba extract in rabbits by UPLC-MS/MS determination. *J Pharm Pharmacol* 2017;69(11):1540–1551.
[39] Jimenez J, Sakthivel M, Nischal KK, et al. Drug delivery systems and novel formulations to improve treatment of rare corneal disease. *Drug Discov Today* 2019;24(8):1564–1574.
[40] Chen J, Zhou R, Li L, et al. Mechanical, rheological and release behaviors of a poloxamer 407/poloxamer 188/carbopol 940 thermosensitive composite hydrogel. *Molecules* 2013;18(10): 12415–12425.
[41] Adibkia K, Selselehjonban S, Emami S, et al. Electrosprayed polymeric nanobeads and nanofibers of modafinil: preparation, characterization, and drug release studies. *Bioimpacts* 2019;9 (3):179–188.
[42] Allam A, El-Mokhtar MA, Elsabahy M. Vancomycin-loaded niosomes integrated within pH-sensitive *in situ* forming gel for treatment of ocular infections while minimizing drug irritation. *J Pharm Pharmacol* 2019;71(8):1209–1221.
[43] Liu S, Cui M, Liu Z, et al. Structural analysis of saponins from medicinal herbs using electrospray ionization tandem mass spectrometry. *J Am Soc Mass Spectrom* 2004;15(2):133–141.
[44] Huhman DV, Sumner LW. Metabolic profiling of saponins in *Medicago sativa* and *Medicago truncatula* using HPLC coupled to an electrospray ion-trap mass spectrometer. *Phytochemistry* 2002;59(3):347–360.
[45] Daull P, Raymond E, Feraille L, et al. Safety and tolerability of overdosed artificial tears by abraded rabbit corneas. *J Ocul Pharmacol Ther* 2018;34(10):670–676.

How to cite this article: Lu P, Wang RX, Xing Y, Gao YQ, Zhang QQ, Xing B, Zhang Y, Yu CX, Cai XF, Shang Q, Kebebe D, Pi JX, Liu ZD. Development and evaluation of *Panax notoginseng* saponins contained in an *in situ* pH-triggered gelling system for sustained ocular posterior segment drug delivery. Acupunct Herb Med. 2021;1(2):107–121. doi: 10.1097/HM9.0000000000000020